

# MODÉLISATION NUMÉRIQUE DE LA MAGNÉTOSTRICION ET DE L'HYSTÉRÉSIS DES MATÉRIAUX MAGNÉTIQUES

H. Vande Sande, G. Deliège, K. Delaere, H. De Gersem, K. Hameyer

Katholieke Universiteit Leuven, Dept. ESAT-ELEN, Kard. Mercierlaan 94, B-3001 Leuven, Belgium

e-mail : hans.vandesande@esat.kuleuven.ac.be

**Résumé** - Pour réaliser des simulations fiables des machines électriques, la modélisation précise des matériaux ferromagnétiques est nécessaire. Des techniques de modélisation de magnétostriction et d'hystérésis sont discutées. L'influence des harmoniques est prise en compte grâce à une approche multi-harmonique.

**Mots clés** - Magnétostriction, Hystérésis, Éléments finis.

## 1. Introduction

Magnetostriction of the stator iron yoke causes stator deformation leading to vibrations and noise. When the material behaviour  $\lambda(B)$  is known (magnetostrictive strain as a function of flux density), the strain distribution can be represented by an equivalent force distribution using the mechanical stiffness matrix of the stator. This way, magnetostriction, reluctance and other external forces can be summed to obtain the total stator deformation.

Hysteresis models have been studied extensively over the past decades. They are however rarely used in commercial software. An implicit use of these models in the harmonic balanced finite element method is discussed in the paper. A short overview of the main properties of these models is given. The saturation of the ferromagnetic core of an inductor model is simulated using the harmonic balanced finite element method.

## 2. Magnetostriction

The deformation caused by magnetostriction (MS) can contribute significantly to the vibrations and noise of electric machinery. Once the  $\lambda(B)$  characteristics of the materials used are known, i.e. magnetostrictive strain  $\lambda$  as a function of magnetic flux density  $B$ , the MS behaviour of the material can be incorporated in the coupled magnetomechanical finite element (FE) analysis. Here, it is illustrated how to take the magnetostrictive strain into account using the thermal stress analogy.

## 3. Coupled magnetomechanical analysis

Because the stator deformation occurring is very small, the coupling between the magnetic FE model and the mechanical FE model is usually effected using a weak coupling (cascade approach). First, the magnetic problem is solved and the reluctance forces and magnetostrictive strain acting on the stator are found by post-processing the magnetic solution. By *magnetostriction forces* we indicate the set of forces that induces the same strain in the material as the magnetostriction effect does. This approach is similar to the use of thermal stresses [1–3]. When all relevant forces have been determined, the mechanical problem is solved, giving the static stator deformations.

## 4. Magnetostriction forces

The finite element method is used to solve for the magnetic field inside a synchronous machine (figure 1), giving the flux density vector  $\vec{B}$  for every element. Then, element by element, the following steps are taken to obtain MS forces:

1. The strain  $\lambda^e$  in the element is determined using the flux density  $B$  in the element. Figure 2 shows a typical magnetostrictive strain versus flux density material characteristic  $\lambda(B)$  for isotropic and anisotropic yoke material.

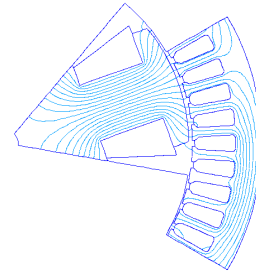


Figure 1: One pole of six-pole synchronous machine: magnetic flux pattern for a particular rotor position.

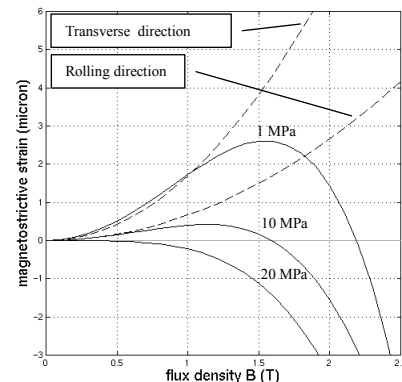


Figure 2: Magnetostrictive material characteristics of non-oriented 3% SiFe (solid lines, as a function of tensile stress) and M330-50A (dashed lines, for rolling and transverse direction).

2. The strains  $\lambda^e$  and  $\lambda_t^e$  are converted into nodal displacements while considering the element's midpoint (centre of gravity) as fixed.

3. For static problems, the mechanical element stiffness matrix  $K^e$  is constructed and multiplied with the MS displacement  $a_{ms}^e$ , yielding the *magnetostriction forces*  $F_{ms}^e = K^e a_{ms}^e$  on the three nodes of the triangular finite element.

Figure 3 shows the  $F_{ms}$  distribution in the yoke of the synchronous machine stator, for the magnetic field shown in figure 1. The MS strain wants to increase the stator circumference. The MS forces can now be added to any external or reluctance forces to give the total force distribution acting on the stator, which can be readily used for deformation or vibration calculation.

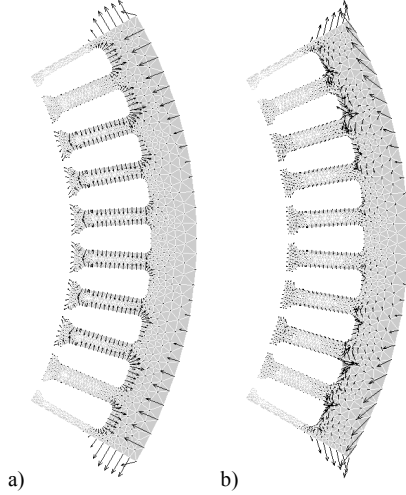


Figure 3: Magnetostriction forces on the stator for  
a) isotropic non-oriented 3% SiFe,  
b) anisotropic M330-50A.

## 5. Non-linear modelling

In modern applications, ferromagnetic materials are operated at substantial levels of saturation and often exhibit significant hysteresis. This results in an increase of the harmonic distortion of all currents and voltages, compared to the harmonic distortion that is already introduced by the power electronic supply and by the motion in the non-homogeneous field of the airgap in the device. FE techniques which allow for static or time-harmonic simulation are widely spread and have proven to be useful in many applications. If e.g. losses have to be predicted, these techniques fail and other approaches have to be considered. An advanced numerical simulation of the machine behaviour requires a comprehensive approach, also taking into account the power supply. Obviously, this seriously increases the complexity of the problem. The incorporation of non-linear and hysteretic material models within finite element simulation is one of the challenging topics in quasistatic electromagnetic simulation. They introduce a sometimes insurmountable burden into the FE software, even if only steady-state operation is considered.

## 6. Multi-harmonic approach

Generally spoken, problems may be studied in time or in frequency domain. In time domain, accurate simulations of the machine, including the power supply, non-linear and hysteretic material characteristics, can be performed by a transient FE analysis. The power supply can be modelled by a function based approach [4]. For hysteresis, numerous techniques have been developed [5,6], among which the models of Preisach, Jiles-Atherton and Stoner-Wolfarth are the most widespread. However, when taking

all these phenomena into account, transient simulations may cause excessive simulation times, especially for models with large meshes or many significant harmonics, to which small time steps have to be applied.

In frequency domain, the time-harmonic approach is commonly applied. However, this technique only allows for the use of one frequency, which limits its applicability. Simultaneous simulation considering more than one frequency, has first been proposed in [8] and is called harmonic balanced FE method (HBFEM). This multi-harmonic approach is not a very common practice, mainly because of the huge computational requirements, both memory and processor time, required to solve the coupled system of equations for all harmonic components in a single step. An iterative solver designed for these particular systems, decreases the simulation times considerably and, hence, enables the application of the multi-harmonic FE method to models of technical devices with complicated geometries and excitations [9].

The HBFEM is especially suited for the simulation of the steady-state operation, as opposite to the transient method which also copes with transient phenomena. However, a fast and accurate simulation of the stationary behaviour is indispensable to detect local hot spots due to additional losses, and the ageing of insulation material due to voltage spikes, during the design process.

The HBFEM can easily be obtained by transforming the governing equation into the frequency domain. Ampère's law in terms of the magnetic vector potential  $\vec{A}$  reads as

$$\nabla \times (\underline{\nu} \nabla \times \vec{A}) + \sigma \frac{\partial \vec{A}}{\partial t} = -\sigma \nabla V \quad , \quad (1)$$

where  $V$  is the applied voltage over the conducting regions with conductivity  $\sigma$  and  $\underline{\nu}$  is the reluctivity. After transformation in the frequency domain, this equation becomes

$$\nabla \times (\underline{\underline{\nu}} * \nabla \times \underline{\underline{A}}) + \underline{\underline{\sigma}} * T(\underline{\underline{A}}) = -\underline{\underline{\sigma}} * \nabla \underline{\underline{V}} \quad , \quad (2)$$

where the magnetic vector potential, the applied voltage, the conductivity and the reluctivity are transformed into discrete spectra. The single bar under the variable represents a spectrum of odd harmonics, while the double bar represents a spectrum of even harmonics. The symbol  $*$  denotes a convolution and  $T$  is the Fourier equivalent operator of the time derivative. In 2D, after discretising the domain in  $n_f$  triangles and writing the solution as a sum of linear FE's for all harmonics

$$\underline{\underline{A}}_z = \sum_{j=1}^{n_f} \underline{\underline{A}}_{z,j} N_j(x,y) \quad , \quad (3)$$

with  $N_j(x,y)$  the shape functions, the following system of equations is obtained:

$$(\underline{\underline{K}} * + \underline{\underline{L}} * T) \underline{\underline{x}} = \underline{\underline{f}} \quad , \quad (4)$$

in which

$$\begin{aligned}
\underline{K}_{ij} &= \int_{\Omega} \underline{\nu} \nabla N_i \cdot \nabla N_j d\Omega \quad , \\
\underline{L}_{ij} &= \int_{\Omega} \underline{\sigma} N_i N_j d\Omega \quad , \\
\underline{x}_j &= \underline{A}_z \cdot j \quad , \\
\underline{f}_i &= \int_{\Omega} \underline{\sigma}^* \nabla V \cdot N_i d\Omega \quad .
\end{aligned}
\tag{5}$$

Often, the conductivity can be considered to be constant, which yields a scalar expression for  $\underline{L}_{ij}$ . Due to the symmetry of the system, a Krylov Subspace is efficiently constructed by the Lanczos procedure. Hence, solvers as Conjugate Gradients or Symmetric Quasi-Minimal Residual are applicable [9,10].

### 7. Saturation

Saturation is taken into account by a non-linear iteration. In each iteration step, the reluctivity spectrum  $\nu(\omega)$ , where  $\omega$  represents the pulsation, has to be determined for every finite element, according to magnetic field spectrum  $B(\omega)$  derived in the previous step. The derivation of these spectra can principally be performed by the following procedure, which is schematically demonstrated in figure 4 ( $T$  is the period of the fundamental component):

1. Calculate  $B(\omega)$  out of  $A_z(\omega)$
2. Transform  $B(\omega)$  into  $B(t)$
3. Calculate  $\nu(t)$  from BH-curve
4. Transform  $\nu(t)$  into  $\nu(\omega)$

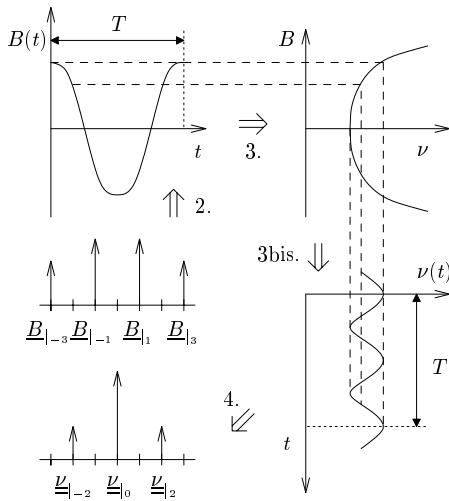


Figure 4: Derivation of the reluctivity spectrum.

This operation is rather time-consuming, as it involves a forward and inverse Fourier transformation. Significant improvements can be achieved by replacing this procedure by a multivariate mapping using standard neural network learning techniques [7]. This mapping can further be optimized by adapting the accuracy to the prescribed accuracy in the non-linear loop.

### 8. Example: inductor with ferromagnetic core

The HBFEM is demonstrated for the simulation of an inductor with a ferromagnetic core (figure 5). The magnetic material only exhibits saturation. A sinusoidal current is applied to the stranded coils and four harmonic components have been considered: the fundamental component, the 3<sup>rd</sup>, the 5<sup>th</sup> and the 7<sup>th</sup> harmonic. Figure 6 shows the field lines for the individual harmonic components.

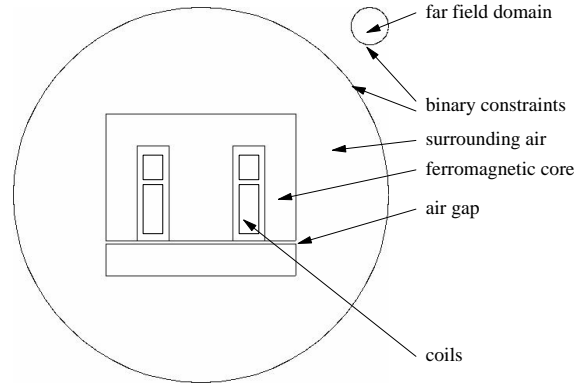


Figure 5: Inductor model with ferromagnetic core.

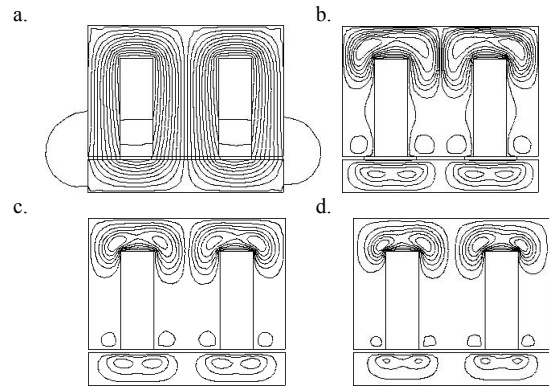


Figure 6: (a-d) Magnetic flux lines of the 1<sup>st</sup>, 3<sup>rd</sup>, 5<sup>th</sup> and 7<sup>th</sup> harmonic component.

The higher harmonic solutions in figure 6 are non physical solutions. There exist closed field lines in regions where no current is present. These plots may not be considered apart from each other. The correct solution is a superposition of the four harmonic components. They however clearly indicate the incidence and importance of saturation.

### 9. Hysteresis

Compared to saturation, hysteresis also introduces a phase difference between the flux density  $\vec{B}$  and the magnetic field strength  $\vec{H}$ . The following constitutive relation holds for hysteretic materials:

$$\vec{H}(t) = \nu(t) \vec{B}(t) + \vec{H}_c(t) \quad , \tag{6}$$

where  $H_c$  represents the coercivity. Here, the reluctivity is assumed to be a scalar. Hence, vectorial equation 6

simplifies to a scalar equation. An extra degree of freedom is introduced, as both the reluctivity  $\nu$  and the coercitive field  $H_c$  are a function of the flux density  $B$ , while  $H_c$  may also be positive or negative depending on the time derivative of the field. The determination of  $\nu$  and  $H_c$  depends on the problem to be solved. One proposal is to define the reluctivity by demanding  $|H_c(B)|$  to be equal, independent of the time derivative of the field.

Ampère's law in terms of the magnetic vector potential is slightly altered in time and frequency domain:

$$\nabla \times (\nu \nabla \times \vec{A}) + \sigma \frac{\partial \vec{A}}{\partial t} = -\sigma \nabla V - \nabla \times \vec{H}_c \quad , \quad (7)$$

$$\nabla \times (\underline{\nu} * \nabla \times \vec{A}) + \underline{\sigma} * \mathbf{T}(\vec{A}) = -\underline{\sigma} * \nabla V - \nabla \times \vec{H}_c \quad . \quad (8)$$

The spectra of the reluctivity and the coercitivity are computed by the same procedure as described for saturation effects, with the help of the hysteresis models, briefly commented below.

## 10. Hysteresis models

The existing hysteresis models can be roughly divided in two different classes: mathematical and physical models [5,6]. Physical models, such as the model of Jiles-Atherton, consider the underlying physics of hysteresis to model the phenomenon. Mathematical models, such as the Preisach model, consider hysteresis as a superposition of elementary hysteresis loops. The Stoner-Wolfarth model is a kind of hybrid model. Recently, hysteresis models based on neural network techniques have been developed [11,12].

The Jiles-Atherton method derives a hysteresis loop out of the Weiss-theory for ferromagnetism. The model relies upon a set of differential equations, for which five parameters have to be determined by a measurement of the hysteresis loop. Despite its simplicity, it can yield a non-physical negative differential permeability and hence lead to numerical instabilities during simulation. Furthermore, higher order loops are not sufficiently well approximated, as opposed to the Preisach model.

In the Preisach model, the hysteresis loop is considered as a superposition of an infinite number of elementary rectangular hysteresis loops, called the Preisach-dipoles. By measuring the Everett-function, a certain weight is assigned to every dipole. Sophisticated Preisach models also comprise dynamical effects and anisotropy. Highly accurate models, however, require the storage of a large amounts of weights.

The Stoner-Wolfarth model also regards the hysteresis loop as a superposition of an infinite number of dipoles. Here, the dipoles themselves can have a non-rectangular hysteresis loops. This model has a lot of numerical disadvantages when compared to the Preisach model. However, it inherits anisotropy thanks to the arbitrarily shaped dipoles.

## 11. Conclusions

Various techniques to model the material behaviour numerically are discussed. The magnetostrictive strains are represented by a set of forces that induce mechanical strains and deformation of the same size as those caused by magnetostriction. Using the FE method, the magnetostriction forces are obtained as a nodal force distribution on the FE mesh. These forces can be used for further deformation or vibration analysis.

A harmonic balanced finite element method is particularly attractive for simulating the steady-state operation of saturated electromagnetic devices, e.g. a ferromagnetic inductor. Hysteresis is incorporated in the approach relying upon well-established hysteresis models, such as the Preisach model, the model of Jiles-Atherton and the Stoner-Wolfarth model.

## Acknowledgement

The authors are grateful to the Belgian "Fonds voor Wetenschappelijk Onderzoek Vlaanderen" and the "Vlaamse Wetenschappelijke Stichting" for the financial support (Project G.0427). Koen Delaere has a FWO-V scholarship. The authors thank the Belgian Ministry of Scientific Research for granting the IUAP No.P4/20 on Coupled Problems in Electromagnetic Systems. The research Council of the K.U.Leuven supports the basic numerical research. Special thanks to R. Mertens for his valuable help in preparing the FE models.

## References

- [1] B.D. Cullity, *Introduction to Magnetic Materials*, in Series in Metallurgy and Materials, Addison-Wesley, Reading, Massachusetts, USA, 1972.
- [2] D. Jiles, *Introduction to Magnetism and Magnetic Materials*, Chapman & Hall, London, UK, 1991.
- [3] L. Hirsinger, *Étude des déformations magnéto-élastiques dans les matériaux ferromagnétiques doux. Application à l'étude des déformations d'une structure de machine électriques*, Ph.D. thesis, Laboratoire de Mécanique et Technologie, Université Paris 6, 1994.
- [4] R. Mertens, U. Pahner, K. Hameyer, "Function Based Approach in Transient Finite Element Analysis", *International Conference on Software for Electrical Engineering Analysis and Design (ELECTROSOFT 99)*, May 17-19, 1999, Sevilla, Spain.
- [5] A. Iványi, *Hysteresis Models in Electromagnetic Computation*, Akademiai Kiado, Budapest, Hungary, 1997.
- [6] I.D. Mayergoyz, *Mathematical Models of Hysteresis*, Springer-Verlag, New York, USA, 1991.
- [7] M. Bishop, *Neural Networks for Pattern Recognition*, Clarendon Press, Oxford, UK, 1995.
- [8] S. Yamada, K. Bessho, J. Lu, "Harmonic Balance Finite Element Method Applied to Nonlinear AC Magnetic Analysis", *IEEE Transactions on Magnetics*, Vol. 25, No. 4, pp. 2971-2973, July 1989.
- [9] H. De Gersem, H. Vande Sande, K. Hameyer, "Strong Coupled Multi-Harmonic Finite Element Simulation Package", *The 9<sup>th</sup> International IGTE Symposium on Numerical Field Calculation in Electrical Engineering (IGTE2000)*, Abstract p. 81, September 11-13, 2000, Graz, Austria.
- [10] H. De Gersem, S. Vandewalle, K. Hameyer, "Krylov Subspace Methods for Harmonic Balanced Finite Element Methods", *Scientific Computing in Electrical Engineering (SCEE2000)*, August 20-23, 2000, Warnemünde, Germany.
- [11] C. Serpico, C. Visone, "Magnetic Hysteresis Modelling via Feed-Forward Neural Networks", *IEEE Transactions on Magnetics*, Vol. 34, pp. 629-635, 1998.
- [12] M. Kuczmann, A. Iványi, "A New Neural Network Model for Magnetic Hysteresis", *The 9<sup>th</sup> International IGTE Symposium on Numerical Field Calculation in Electrical Engineering (IGTE2000)*, Abstract p. 98, September 11-13, 2000, Graz, Austria.